



Spatial variation in mercury concentrations in polar bear (*Ursus maritimus*) hair from the Norwegian and Russian Arctic



Anna Lippold^{a,1}, Andrei Boltunov^b, Jon Aars^a, Magnus Andersen^a, Marie-Anne Blanchet^{a,c}, Rune Dietz^d, Igor Eulaers^{a,d}, Tamara N. Morshina^e, Vyacheslav S. Sevastyanov^f, Jeffrey M. Welker^{g,h,i}, Heli Routti^{a,*}

^a Norwegian Polar Institute, Fram Centre, Tromsø 9296, Norway

^b Marine Mammal Research and Expedition Centre, 36 Nahimovskiy pr., Moscow 117997, Russia

^c UiT The Arctic University of Norway, Tromsø 9019, Norway

^d Aarhus University, Institute of Ecoscience, Arctic Research Centre, Roskilde 4000, Denmark

^e Research and Production Association "Typhoon", 249038 Obninsk, Kaluga Region, Russia

^f Vernadsky Institute of Geochemistry and Analytical Chemistry RAS, Moscow 119991, Russia

^g University of Alaska Anchorage, Anchorage 99508, United States

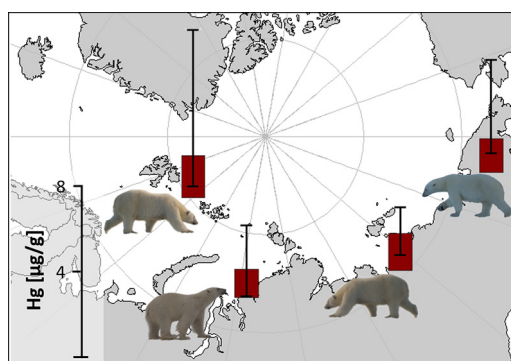
^h University of Oulu, Oulu 90014, Finland

ⁱ University of the Arctic, Rovaniemi 96460, Finland

HIGHLIGHTS

- We examined total Hg (THg) concentrations in 100 polar bear hair samples.
- The samples were from Barents Sea, Kara Sea, Laptev Sea, and Chukchi Sea.
- THg levels in the Norwegian and Russian Arctic were relatively low.
- Spatial variation in THg concentrations were not related to feeding ecology.

GRAPHICAL ABSTRACT



ARTICLE INFO

Article history:

Received 15 September 2021

Received in revised form 26 January 2022

Accepted 27 January 2022

Available online 2 February 2022

Editor: Rafael Mateo Soria

Keywords:

Hg
Stable isotopes
Svalbard
Kara Sea
Chukchi Sea

ABSTRACT

We examined spatial variation in total mercury (THg) concentrations in 100 hair samples collected between 2008 and 2016 from 87 polar bears (*Ursus maritimus*) from the Norwegian (Svalbard Archipelago, western Barents Sea) and Russian Arctic (Kara Sea, Laptev Sea, and Chukchi Sea). We used latitude and longitude of home range centroid for the Norwegian bears and capture position for the Russian bears to account for the locality. We additionally examined hair stable isotope values of carbon ($\delta^{13}\text{C}$) and nitrogen ($\delta^{15}\text{N}$) to investigate feeding habits and their possible effect on THg concentrations. Median THg levels in polar bears from the Norwegian Arctic ($1.99 \mu\text{g g}^{-1}$ dry weight) and the three Russian Arctic regions ($1.33\text{--}1.75 \mu\text{g g}^{-1}$ dry weight) constituted about 25–50% of levels typically reported for the Greenlandic or North American populations. Total Hg concentrations in the Norwegian bears increased with intake of marine and higher trophic prey, while $\delta^{13}\text{C}$ and $\delta^{15}\text{N}$ did not explain variation in THg concentrations in the Russian bears. Total Hg levels were higher in northwest compared to southeast Svalbard. $\delta^{13}\text{C}$ and $\delta^{15}\text{N}$ values did not show any spatial pattern in the Norwegian Arctic. Total Hg concentrations adjusted for feeding ecology showed similar spatial trends as the measured concentrations. In contrast, within the Russian Arctic, THg levels were rather

* Corresponding author at: Norwegian Polar Institute, Fram Centre, Postboks 6606 Stakkevollan, 9296 Tromsø, Norway.

E-mail address: heli.routti@npolar.no (H. Routti).

¹ Present address: Department of Biology, McGill University, Montreal, Quebec, H3A 1B1, Canada

uniformly distributed, whereas $\delta^{13}\text{C}$ values increased towards the east and south. The results indicate that Hg exposure in Norwegian and Russian polar bears is at the lower end of the pan-Arctic spectrum, and its spatial variation in the Norwegian and Russian Arctic is not driven by the feeding ecology of polar bears.

1. Introduction

Mercury (Hg) is a naturally occurring element released by rock weathering or volcanic activity (Fitzgerald and Lamborg, 2007). However, its atmospheric concentrations have increased 6 to 8-fold since the onset of the anthropogenic era in the 15th century AD due to mining, coal burning and other industrial processes (Outridge et al., 2018). This observation of anthropogenic increase of circulating Hg is joined by observations of a 10-fold increase of Hg levels in hard tissues (teeth, hair, feathers) of Arctic marine animals from the mid- to late-19th century (Dietz et al., 2009). Polar bears (*Ursus maritimus*) are circumpolar apex predators, which are exposed to high levels of bioaccumulative pollutants such as Hg, which potentially lead to adverse health effects (Muir et al., 1999; Braune et al., 2005; Dietz et al., 2013; Dietz et al., 2019). Hg concentrations reportedly differ up to tenfold across polar bear subpopulations (Rush et al., 2008; Routti et al., 2011). Such spatial variation could be driven by Hg emission patterns and by a plethora of environmental processes, such as long-range transport, atmospheric precipitation and depletion events, and Hg bioavailability and methylation, as well as by variation in polar bear body condition and feeding ecology coupled to food web length and dynamics (St. Louis et al., 2011; Kirk et al., 2012; Routti et al., 2012; McKinney et al., 2017; Wang et al., 2018).

Patterns of Hg emission, its distribution and concentrations in the abiotic and biotic environment depict a complicated combination of various processes. From the local point of emission, Hg is transported to remote places, such as the Arctic, via atmospheric, riverine and ocean currents (Kirk et al., 2012; Outridge et al., 2018). In the Arctic, only an estimated 2% of deposited anthropogenic Hg stem from point source emissions, while the main proportions of Hg deposited in the Arctic come from Asia (Kirk et al., 2012; UN Environment, 2019). Within the Arctic, Hg concentrations in the atmosphere, surface snow and meltwater can vary by several orders of magnitude spatially and seasonally due to differences in atmospheric Hg depletion events, reemission from the snow pack, tundra and oceans, and variation of long-range transport episodes (Kirk et al., 2012). Higher levels of Hg in the Arctic Ocean compared to adjacent oceans can be attributed to high freshwater inputs from the immense rivers that drain vast regions of North America and Eurasia into the Arctic such as the MacKenzie, Ob, Lena, Yenisey and others (Soerensen et al., 2016), which has been linked to Hg levels in polar bears from the Alaskan and Canadian Arctic and Greenland (Routti et al., 2012). Hg evasion occurs over the continental shelf areas, whereas sea ice cover limits Hg evasion in the Arctic Basin (Soerensen et al., 2016; Sonke et al., 2018).

A small fraction [4–14% in Arctic marine waters (Kirk et al., 2012)] of the Hg present in the environment is transformed by bacteria to monomethyl-mercury (MeHg), a species of Hg that is neurotoxic, readily accumulates in organisms by binding to proteins, and biomagnifies through food webs (reviewed by Kirk et al., 2012; AMAP, 2011; Lehnher, 2014)). Factors that might influence MeHg levels in top predators such as polar bears are, for example, microbial processes, environmental sulfate concentrations, vertical profiles of subsurface MeHg in sea water, uptake, and biomagnification at low trophic levels (Benoit et al., 2002; Jeremiason et al., 2006; Elliott and Elliott, 2016; Gongora et al., 2018; Wang et al., 2018; Schartup et al., 2020; Zhang et al., 2020). For example, higher concentrations of THg in polar bears from the southern Beaufort Sea compared to those from the western Hudson Bay were related to higher concentrations of pelagic MeHg and a longer more pelagic food web in the southern Beaufort Sea (St. Louis et al., 2011). The availability of Hg to food webs can also be affected by sea ice. Particularly high MeHg concentrations were observed just below the productive surface layer in the marginal ice zone, which likely enhances uptake and bioavailability of MeHg in food webs

(Heimburger et al., 2015). A circumpolar study on polar bears also suggested higher Hg levels in polar bear food webs rich in copepods that are abundant in marginal ice zones (Routti et al., 2012; Daase et al., 2013). Additionally, climate change has potentially far-reaching impacts on Hg and MeHg concentrations in the Arctic environment as well as in top predators. For example, climate change could lead to increased re-emissions from melting sea-ice, glaciers, and permafrost; or to changes in Hg methylation and demethylation rates (Kirk et al., 2012; Stern et al., 2012; Elliott and Elliott, 2016). Changes in atmospheric or oceanic Hg distribution, deposition or forms; or changes in food webs or body condition might also affect polar bear exposure to Hg (Kirk et al., 2012; Stern et al., 2012), and will likely vary spatially.

Circumpolar Hg trends inferred from polar bears have mainly been conducted on subpopulations from North America and Greenland (Norstrom et al., 1986; Born et al., 1991; Braune et al., 1991; Rush et al., 2008; Routti et al., 2011). Studies based on samples collected over the years 2005–2008 suggest that polar bears from the Beaufort Sea are exposed to very high levels of Hg compared to other subpopulations, which was related to high riverine input of terrestrial carbon in that area (Routti et al., 2012). Although the Russian Arctic together with the Norwegian Arctic covers half of the coastline of the Arctic Ocean, reports about Hg concentrations in polar bears from that region are scarce (Renzoni and Norstrom, 1990; Routti et al., 2019). Knowledge on exposure to mercury and other pollutants in polar bears is highly important as contaminant exposure is considered as one of the largest threats to polar bears after climate change (Polar Bear Range States, 2015). Long term consequences of polar bears' habitat degradation which is particularly rapid in the Barents Sea, are currently not known for polar bear subpopulations from the Russian and Norwegian Arctic (www.pbsg.npolar.no).

To better understand the spatial distribution of THg in polar bears, we examined THg concentrations in polar bear hair from the Norwegian Arctic (Svalbard in the Barents Sea) and Russian Arctic (Kara Sea, Laptev Sea, and Chukchi Sea). Additionally, we related hair THg concentrations to individual polar bear feeding ecology, approximated by stable isotope values for carbon ($\delta^{13}\text{C}$, representing carbon source) and nitrogen ($\delta^{15}\text{N}$, representing trophic position), and biological parameters such as breeding status, body condition index (BCI) and age, whenever this information was available. We also investigated spatial variation in stable isotope values and their impact on spatial trends of THg in polar bears. Total Hg concentrations, stable isotope values, BCI, breeding status, and age for the bears of the Norwegian Arctic have already been reported earlier with yearly resolution as a part of a larger temporal trend study spanning from 1995 to 2016 (Lippold et al., 2020a), but a subset (bears sampled in 2011–2016 with telemetry data) of the data (Lippold et al., 2020b) is used herein to study spatial variation of THg with and without adjustments to dietary/biological parameters. This subset of bears with telemetry data allowed us to study THg concentrations in relation to space use in the Barents Sea polar bears.

2. Materials and methods

2.1. Sample collection

Hair samples were collected from polar bears from Svalbard in the Barents Sea ("Norwegian Arctic"), and from the Kara Sea, Laptev Sea, and Russian side of the Chukchi Sea ("Russian Arctic"; see Fig 1). The details of sample collection in the Norwegian Arctic are described elsewhere (Lippold et al., 2020a). Briefly, 42 hair samples were collected from 29 adult (>4 years) female polar bears captured in spring between 2011 and 2016, of which 9 were sampled more than once (captured bears are individually marked). The hair was cut close to the skin

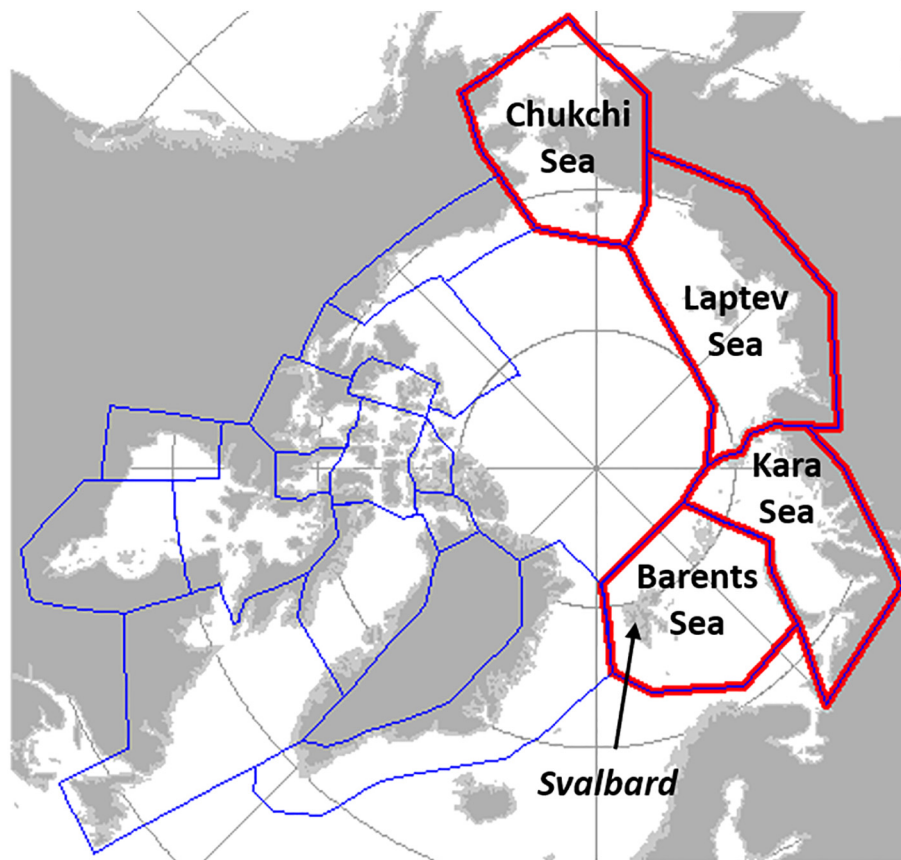


Fig. 1. Polar bear subpopulation boundaries (blue and red lines). Areas with red borders are included in this study.

approximately 10 cm lateral to the base of the tail. The bears were immobilized by remote injection of tiletamine and zolazepam hydrochloride (Zoletil Forte Vet, Virbac, France) (Stirling et al., 1989). All bears were weighed in the field and the body condition index (BCI) was calculated accordingly: $BCI = (\ln(\text{body mass}) - 3.07 * \ln(\text{length}) + 10.76) : (0.17 + 0.009 * \ln(\text{length}))$ (Cattet et al., 2002). Age estimation was derived from growth rings in vestigial premolar teeth (Christensen-Dalsgaard et al., 2009), or if bears had earlier been captured as cubs, their known age was used. Breeding status, i.e. with yearlings, with cubs of the year, or solitary, was recorded. The permits for sampling in the Norwegian Arctic were obtained from the Norwegian Food Safety Authority and the sampling was carried out in accordance with relevant guidelines and regulations from the Governor of Svalbard.

The sampling of polar bear hair ($n = 58$) from the Russian Arctic was conducted during a number of expeditions from late March to early October (except one sample collected in January) between 2008 and 2016. The samples were collected either from immobilized animals ($n = 33$) as described above or opportunistically from carcasses ($n = 21$) or shed hair ($n = 4$). Collection of the samples from immobilized animals occurred either in spring (17th April–12th June, $n = 13$) or in autumn (23rd August and 6th October, $n = 20$). Most of the samples collected from carcasses or shed hair was done in autumn. The immobilization was approved by the Russian Federal Supervisory Natural Resources Management Service.

Hair was used as non-lethal proxy to study spatial variation in THg concentrations and stable isotope values of carbon and nitrogen. Polar bear guard hair is expected to grow during summer and autumn (Born et al., 1991; Rogers et al., 2015). Trace elements and stable isotope values in polar bear guard hair collected from rump are believed to represent Hg, nitrogen and carbon intake during or preceding the period of hair growth (Born et al., 1991; Rogers et al., 2015; Rode et al., 2016; Bechshoft et al., 2020).

2.2. Determination of locality

The categorization of each sample into subpopulations was based on home-range centroids or the site of capture. Boundaries of the relatively distinct subpopulations also define boundaries of polar bear management units recognized by international management plans (Figure 1) (Polar Bear Range States, 2015). Twenty-nine bears from the Norwegian Arctic were equipped with telemetry devices used to assign each bear to a specific area within this region. The bears were equipped with Global Positioning System (GPS) satellite transmitters type TGW-4678-3 or TGW-4678-4 from Telonics (Mesa, AZ, USA), Sirtrack Prox (Havelock North, New Zealand) or Advanced Telemetry Systems (ATS) Iridium (Isanti, MN, USA). A bear's core area was defined as 50% of their home ranges estimated using the minimum convex polygon method (Mohr, 1947). We used this definition to focus on an area representative of where bears would spend most of their time and avoid the bias linked to outlier locations. Locations collected during denning were removed. We then calculated the geographic position of the core area using the polygon's centroid. If a bear had data from two or more years, in some cases from more than one collar, we averaged the yearly centroid positions (Blanchet et al., 2020). The hair sampling occurred either when a bear was equipped with a collar or within a 1 to 5 years period preceding or following the collaring. Thus, the centroid position was not necessarily determined for the period when the bears were assumed to accumulate Hg. However, polar bears in the Barents Sea region have a stable space-use strategy across years especially for bears of the coastal ecotype that made up 24 out of our 29 samples (Mauritzen et al., 2001; Tartu et al., 2018; Blanchet et al., 2020; Brun et al., 2021). A recent study shows that the intra-individual variation in home range centroid is only 15 km on average in coastal polar bears (Brun et al., 2021). This centroid position was therefore likely representative of the area used by a bear and where Hg was accumulated.

We did not have telemetry data for the bears captured from the Russian Arctic. Therefore, we used latitude and longitude of the capture position to account for the locality of these bears. This choice was supported by the fact that the centroid home range position of the Norwegian polar bears correlated highly with their capture position (latitude $r = 0.89$, longitude $r = 0.94$; Fig. A1).

2.3. Hg analysis

The analysis for total Hg (THg) in the polar bear hair samples collected in the Norwegian Arctic is described elsewhere in detail (Lippold et al., 2020a). Briefly, for the THg analysis, the entire shaft of the hair was used and homogenized with scissors. Prior to analysis, the hair was washed in a diluted standard detergent (RBS 35; Bie & Berntsen A/S, Denmark), rinsed in several ultra-pure Milli-Q water baths, and dried for 24 h at room temperature. Total Hg concentrations in a subsample of 5–10 mg of polar bear hair were analyzed at the accredited trace element laboratory of the Aarhus University, Denmark, using a Milestone DMA-80 Direct Mercury Analyzer. The analytical quality was tested by analyzing 14 samples of Certified Reference Material, being dogfish liver (DOLT-5), five duplicates of polar bear hair samples and four samples of working standard containing 10 ppm of Hg. The recoveries of Hg in the CRM DOLT-5 samples ranged from 92 to 99% (median 94%) and were within the acceptable range of the certified value of $0.44 \pm 0.18 \mu\text{g g}^{-1}$ dry weight. The coefficient of variation of 3.2% for DOLT-5 and the relative percent differences for the duplicate analyses of polar bear samples (median 1.18%, range 0.27–9.9%) confirmed the precision of the analyses.

Moreover, the trace element laboratory of the Aarhus University participates twice a year in the international laboratory performance study program QUASIMEME (www.quasimeme.org), which documents excellent long-term measurement accuracy ($n = 9$ during 2017–2019; assigned concentration from 0.009 to 0.951 mg kg^{-1} dw; Z-scores ranged from -1.0 to 0.6 with a mean of 0.0).

Polar bear hair samples collected in Russia were analyzed for THg by Typhoon, Federal Service for Hydrometeorology and Environmental Monitoring. The hair samples ($n = 58$) were analyzed for THg according to the method RD 52.18.827–2016 entitled “Mass fraction of mercury in soil, sediment, and biological samples analyzed by cold vapor atomic absorption spectrometry” (<http://docs.cntd.ru/document/556459506>; in Russian). Briefly, samples of 0.5–5.0 g of dry polar bear hair were washed first with acetone and then by distilled water and dried in air. The hair samples were homogenized with scissors and mixed. Concentrated high purity nitric acid (1 mL; GOST 11125-84), perchloric acid (1 mL; MRTU 6-09-6604-70) and sulfuric acid (5 mL; GOST 14262-78) sourced from Himmed Sintez (Moscow, Russia) were added to each sample of 0.20 ± 0.02 g of hair. The mixture was heated to 180–210 °C for 20 min, cooled down and 15% potassium permanganate was added (1–3 mL until a persistent pale pink colour appeared). The solution was filtered and diluted with water to a volume of 25 mL. The quantification was conducted using an Atomic Absorption Spectrometer Varian AA 140 at 253.6 nm (Varian, Palo Alto, CA, USA – verification certificate N. 13, valid until 21.01.2020) equipped with a vapor generation assembly VGA 77. A 30% solution of tin(II) chloride in hydrochloric acid (1:1) was used as a reducing agent. The instrument was calibrated using calibration solutions with Hg concentrations of 5.0, 10.0 and 20.0 $\mu\text{g/L}$. Calibration solutions contained 12 mL of hydrochloric acid and 6 mL of nitric acid per 100 mL of solution. Calibration solutions were prepared on the day the samples were measured. The operational quality control of the analyses was carried out using a standard addition method, where a subsample was spiked with a lower amount of Hg standard than found in the sample. Accuracy was assessed by analyzing THg concentrations in one CRM sample (fish protein DORM-4), which deviated $+1.7\%$ from the assigned value of $0.412 \pm 0.036 \mu\text{g g}^{-1}$ dry weight. The relative percent difference of duplicate analysis of one polar bear sample (14.4%) was used to assess the analytical precision.

Five hair samples were analyzed at both participating labs to assess comparability. The median relative percent difference of the duplicate

analyses was 14.3% (range: 4.4 to 39%), which corresponds $0.12 \mu\text{g g}^{-1}$ dw (median; range: 0.06 – $1.79 \mu\text{g g}^{-1}$ dw) (Table 1).

2.4. Stable isotope analysis

Details for the stable carbon and nitrogen isotope analysis in hair from polar bears from the Norwegian Arctic are available elsewhere (Lippold et al., 2020a). Briefly, the entire hair shafts were homogenized with scissors and washed with 2:1 chloroform-methanol solution prior to analysis; and the stable isotope analysis was conducted in a subsample of 1 mg using a Costech ECS 4010 elemental analyzer (Costech, Valencia CA) in line with a Thermo Finnigan DeltaPlus XP continuous-flow isotope ratio mass spectrometer (Thermo Scientific, Bremen, Germany) at the University of Alaska Anchorage Stable Isotope Laboratory, USA, for all samples from 2011 to 2013 and 2015–2016. Samples from 2014 were analyzed at the Trophic Ecology Laboratory at the University of Windsor's Great Lakes Institute for Environmental Research, Windsor, Canada, using a Delta V Advantage ThermoScientific Continuous Flow Mass Spectrometer (Thermo Scientific, Bremen, Germany) coupled to a 4010 Elemental Combustion System (Costech Instruments, Valencia, CA, USA). Long-term records of internal standards yield an analytical precision of 0.1‰ for $\delta^{13}\text{C}$ and 0.2‰ for $\delta^{15}\text{N}$ at the University of Alaska Anchorage Stable Isotope Laboratory, and a precision of 0.2‰ for both $\delta^{13}\text{C}$ and $\delta^{15}\text{N}$ at the Trophic Ecology Laboratory at the University of Windsor (for details, see Lippold et al., 2020). Median absolute deviation of duplicate analyses of polar bear hair samples ($n = 7$ pairs) at the University of Alaska Anchorage was 0.55‰ (range 0.00 – 3.22‰) for $\delta^{15}\text{N}$ and 0.20‰ for $\delta^{13}\text{C}$ (range: 0.17 – 0.47‰).

The polar bear hair samples from the Russian Arctic were analyzed for stable isotopes at the Vernadsky Institute of Geochemistry and Analytical Chemistry, Russian Academy of Sciences, Moscow. Before the analysis, the hair samples were cleaned from any traces of adhering organic residue in a three times repeated procedure of two 30 min ultrasonic baths of first 2:1 chloroform-methanol mixture and subsequently distilled water. The samples were then dried in a drying cabinet at 80 °C for 12 h. The isotopic composition of carbon in the samples was determined using a Delta-Plus XP Isotope Ratio Mass Spectrometer (Thermo Fisher Scientific, Bremen, Germany) coupled to a Flash EA 1112 Element Analyzer (Thermo Scientific, Germany). The mass of the analyzed samples was 0.2 mg. The analytical precision was assessed by including samples of the international reference materials. $\delta^{13}\text{C}$ value in NBS 22 Oil (RM8539, National Institute of Standards and Technology) was within 0.33‰ of the reference value

Table 1

THg concentrations and stable isotope values in polar bear hair analyzed in two different Results from analyses of duplicate polar bear samples in Denmark and Russia.

	Denmark (THg)/Alaska US ($\delta^{15}\text{N}$, $\delta^{13}\text{C}$)	Russia	Difference
THg in bear #26102 ($\mu\text{g g}^{-1}$ dry weight)	0.76	0.82	-0.06
THg in bear #23699 ($\mu\text{g g}^{-1}$ dry weight)	2.25	1.84	0.41
THg in bear #23637 ($\mu\text{g g}^{-1}$ dry weight)	3.67	5.46	-1.79
THg in bear #23945 ($\mu\text{g g}^{-1}$ dry weight)	2.75	2.63	0.12
THg in bear #23732 ($\mu\text{g g}^{-1}$ dry weight)	1.3	1.13	0.17
$\delta^{15}\text{N}$ in bear #26102 (‰)	16.99	15.35	1.64
$\delta^{15}\text{N}$ in bear #23945 (‰)	18.04	16.92	1.12
$\delta^{15}\text{N}$ in bear #23966 (‰)	17.34	15.99	1.35
$\delta^{15}\text{N}$ in bear #23637 (‰)	18.35	16.64	1.71
$\delta^{15}\text{N}$ in bear #23732 (‰)	19.01	16.05	2.96
$\delta^{13}\text{C}$ in bear #26102 (‰)	-18.18	-18.4	0.22
$\delta^{13}\text{C}$ in bear #23945 (‰)	-17.19	-15.77	-1.42
$\delta^{13}\text{C}$ in bear #23966 (‰)	-17.32	-17.15	-0.17
$\delta^{13}\text{C}$ in bear #23637 (‰)	-16.5	-19.14	2.64
$\delta^{13}\text{C}$ in bear #23732 (‰)	-16.92	-17.87	0.95

(reference value: $-30.03 \pm 0.09\%$, measured value: -29.7%). $\delta^{15}\text{N}$ values in IAEA-NO-3 (International Atomic Energy Agency) were within the accepted range (reference value $4.7 \pm 0.2\%$, measured values $4.56\text{--}4.86$ [$n = 5$]).

To assess the comparability of the results from the labs in Anchorage and Moscow, 5 hair samples from Norwegian bears were analyzed in both labs. The median absolute deviation between the results was 0.95% (range $0.17\text{--}2.64\%$) for $\delta^{13}\text{C}$, and 1.64% (range $1.12\text{--}2.96\%$) for $\delta^{15}\text{N}$ (Table 1). Owing to these differences, the results were treated separately in statistical analysis and discussion.

2.5. Statistical analyses

The dataset is available in the Norwegian Polar Data Centre repository (Routti et al., 2021). The statistical analyses were conducted using R version 3.6.1 (R Core Team, 2019). The spatial variation of the measured THg concentrations and stable isotope values were displayed using the ggplot function (package ggplot2 (Wickham, 2016) in combination with the packages GGally (Schloerke et al., 2018), maps (Becker et al., 2018), and mapproj (McIlroy, 2018).

We used one-way ANOVA and post hoc Tukey's test to compare log-transformed THg concentrations among the subpopulations.

The effect of centroid home range or capture position and feeding ecology (approximated by $\delta^{13}\text{C}$ and $\delta^{15}\text{N}$) on the hair THg concentrations were investigated using generalized additive (mixed) models (GAMM for the Norwegian Arctic to account for repeated captures; GAM for the Russian Arctic) using the R packages mgcv (Wood, 2018), lme4 (Bates et al., 2015), and nlme (Pinheiro et al., 2019) with a gamma distribution and identity link for the response variable. We additionally included breeding status, BCI and age as covariates for the analyses of the Norwegian bears. We analyzed the bears from the Norwegian Arctic separately from the bears from the Russian Arctic due to differences in covariate availability and variability in the results from the different laboratories. For the Norwegian polar bears we defined 10 models that each included a smoothed variable for centroid home range position (te(Latitude, Longitude)) except for a null model (THg ~ 1), and additionally $\delta^{13}\text{C}$, $\delta^{15}\text{N}$, breeding status, BCI, and age as linear predictor variables (Table A1). All models included polar bear ID as a random factor to account for recaptures. For the Russian bears, we defined four candidate models with $\delta^{13}\text{C}$ or $\delta^{15}\text{N}$ in addition to the smoothed capture position as linear predictor variables (Table A1). As the Russian capture positions included negative longitudes, we transformed these (longitude + 360) to avoid a discontinuous interpretation of the longitude variable. None of the Russian bears were recaptured, thus no random effect was included. Although the Russian samples were from both males and females, we did not include sex as a predictor, since the information on sex was available only from a subset of the Russian bears. However, exploratory analyses showed no significant effect of sex on THg concentrations in the Russian bears (male [$n = 23$] vs. female [$n = 19$] -0.13 , 95% confidence interval [CI]: $-0.57, 0.31$; GAM).

Values for BCI, $\delta^{13}\text{C}$ and $\delta^{15}\text{N}$ were normalized using the Z-score method ($Z = \text{value} - \text{mean}/\text{standard deviation (SD)}$; leading to mean = 0 and $SD = 1$ for all features) to aid comparison between effect sizes. Values for $\delta^{13}\text{C}$ and $\delta^{15}\text{N}$ were not included in the same models to avoid collinearity (Norwegian Arctic: $r = 0.58$, Russian Arctic: $r = 0.37$). We used the model.sel() function of the R package MuMIn (Barton, 2019) to rank and weigh all candidate models based on Akaike's Information Criterion (Table 3), and finally average model estimates based on their weights (Table 3). One of the Norwegian bears had the centroid home range position far out in the Barents Sea and was considered an outlier and excluded from all statistical analysis (Fig. A2). Diagnostic plots of model residuals ensured model assumptions (i.e. homogeneity, model fit, and normality of residuals) were not violated (Fig. A3).

We also used models in which latitude and longitude were linear predictors of THg or the diet proxies, to quantify latitudinal and longitudinal trends using generalized linear (mixed) models (glm(er)) with a gamma distribution and identity link for THg. We used these models

to explore potential differences in latitudinal or longitudinal trends between the above-mentioned models with and without biological predictors (Hg \sim latitude or longitude + $\delta^{13}\text{C}$ + breeding status; and Hg \sim latitude or longitude) to understand the effect of feeding ecology and breeding status on the spatial trends of THg. To quantify spatial trends of stable isotope values, we used GAM(M)s with te(Lat, Lon) as predictor for both $\delta^{13}\text{C}$ and $\delta^{15}\text{N}$, and additionally breeding status for $\delta^{15}\text{N}$, as it helped explain variation in $\delta^{15}\text{N}$.

3. Results and discussion

We analyzed THg in hair samples of a total of 100 polar bears from the Norwegian and Russian Arctic. Hair THg concentrations in polar bears correlate moderately with concentrations in muscle, kidney and blood ($0.4 < r < 0.5$), whereas correlations between hair and liver are stronger ($r = 0.69$) (Born et al., 1991; Cardona-Marek et al., 2009; Bechshoft et al., 2019). Thus, hair is a useful matrix for THg analysis, as it is non-invasive and reflects liver concentrations. Furthermore, potential differences in sampling period are not likely to lead to any systematic error in data interpretation, since the variation in THg concentrations along guard hair length is not consistent among individuals (Bechshoft et al., 2020).

In the three Russian populations (Kara Sea, Laptev Sea, and Chukchi Sea), median hair THg concentrations ranged from 1.33 to $1.75 \mu\text{g g}^{-1}$ dw, with a minimum of 0.04 and a maximum of $5.33 \mu\text{g g}^{-1}$ dw (Table 2; Figure 2). Hair THg concentrations in polar bears from the Norwegian Arctic ranged from $0.53\text{--}7.94 \mu\text{g g}^{-1}$ dw, with a median of $1.99 \mu\text{g g}^{-1}$ dw (Table 2; Figure 2). The only significant subpopulation difference was observed between the Norwegian Arctic and the Kara Sea with $0.78 \mu\text{g g}^{-1}$ dw (95% CI: $0.13, 1.43$) higher THg concentrations in the former one. The subpopulation comparison between the Norwegian and Russian bears should be interpreted with caution due to the variability in the results from the laboratories analyzing the Norwegian and Russian samples (Table 1). However, the median variation between the laboratories ($0.12 \mu\text{g g}^{-1}$ dw) was only 15% of the difference in Hg concentrations between the Norwegian and the Kara Sea bears and even smaller compared to the differences among circumpolar subpopulations (Table 4; Routti et al., 2019). Yet, the inter-laboratory differences between some paired samples were higher (Table 1) and we thus want to emphasize to take caution when interpreting minor differences among Hg concentrations at circumpolar level, both in the present study on the Norwegian and Russian Arctic as well as other international studies including several subpopulations. Hair THg concentrations in the Norwegian and Russian bears were generally lower than those in the bears from Greenland and North-American Arctic based on comparisons of geometric means (Table 4; Routti et al., 2019). This circumpolar spatial study (i.e. Routti et al., 2019) included a small subset of samples from the Barents Sea, Kara Sea and Chukchi Sea subpopulations also used in the present study and suggested particularly high Hg concentrations in East Greenland polar bears. The hair concentrations of THg in the present study were also lower than concentrations recently reported for Baffin Bay and Western Hudson Bay (Yurkowski et al., 2020; Stern et al., 2021). Renzoni and Norstrom (1990) also reported lower THg concentrations in polar bear hair from the Russian Arctic compared to those from the Canadian Arctic and Svalbard.

Models (GAMM) suggested a significant non-linear spatial THg trend within the polar bears from the Norwegian Arctic (Table 2), with higher levels in the Northwest than the Southeast (Figure 3). AIC model ranking showed $\delta^{13}\text{C}$ in combination with centroid home range position and breeding status as most important predictors for THg concentrations (Table 3A). Total Hg concentrations increased with $\delta^{13}\text{C}$ and $\delta^{15}\text{N}$, suggesting a higher proportion of marine prey and feeding at a higher trophic position leading to higher hair THg concentrations. Our results suggested marginally higher hair THg concentrations in females with yearlings than solitary females (Table 3A), which is in accordance with a recent study with a larger dataset from the Norwegian Arctic and a study from Baffin Bay (Lippold et al., 2020a; Stern et al., 2021). Total Hg concentrations were not significantly related to BCI or age in polar bears from the Norwegian Arctic

Table 2

Numbers of samples, median (mEd.), minimum and maximum THg concentrations ($\mu\text{g g}^{-1}$ dw) and stable isotope values (‰ unit) for carbon ($\delta^{13}\text{C}$) and nitrogen ($\delta^{15}\text{N}$) in hair from polar bears from Svalbard, Kara Sea, Laptev Sea and Chukchi Sea as well as numbers of males, females, and bears of unknown sex and bears of different age groups. Body condition index (BCI; arbitrary units) and age (years) distribution is shown if the data was available.

		Svalbard/Norwegian Arctic	Kara Sea	Laptev Sea	Chukchi Sea
<i>n</i>		41	31	7	20
Year		2011–2016	2012–2016	2014–2016	2008–2016
THg	med	1.99	1.33	1.75	1.6
	min-max	(0.53–7.94)	(0.04–3.4)	(0.73–2.99)	(0.9–5.33)
$\delta^{13}\text{C}$	med	–18.03	–18.53	–18.9	–16.15
	min-max	(–20.28 to –16.92)	(–22.59 to –17.2)	(–19.72 to –18.69)	(–20.08 to –14.53)
$\delta^{15}\text{N}$	med	16.65	16.31	15.76	16.42
	min-max	(13.95–19.09)	(14.33–17.33)	(15.12–16.01)	(13.22–17.81)
Sex	m	0	17	1	5
	f	29 (11 recaptures)	10	5	4
	?	0	4	1	11
BCI	med	–1.68			
	min-max	(–3.1 – 0.27)			
Age group	adult	41	20	4	7
	subadult		4	1	3
	cub		5	1	2
	unknown		2	1	8
Age	med	9			
	min-max	5–21			

(Table 3A), an observation contrary to e.g. (McKinney et al., 2017), who found decreasing hair THg levels with increasing body mass. Total Hg concentrations adjusted for $\delta^{13}\text{C}$ and breeding status had a similar spatial trend to the measured concentrations (Figure 3).

When we separated latitude and longitude and assessed their respective effect on THg concentrations with (0.45 [CI: 0.08, 0.83] for latitude, and –0.12 [CI: –0.21, –0.02] for longitude) and without (0.58 [CI: 0.12, 1.04] for latitude, and –0.16 [CI: –0.27, –0.05] for longitude) additional predictors ($\delta^{13}\text{C}$ and breeding status according to GAMM model selection), the estimates from the full model and the parsimonious model without biological predictors hardly differed. This suggests that the variation in carbon source (marine vs. terrestrial) only had a very minor influence on the spatial variation in THg concentrations in the polar bears from the Norwegian Arctic.

The variation for both $\delta^{13}\text{C}$ and $\delta^{15}\text{N}$ did not follow any significant spatial trend in polar bears from the Svalbard archipelago (Figures 3, significance of *te* (Lat, Lon) for $\delta^{13}\text{C}$: $P = 0.70$, $\delta^{15}\text{N}$: $P = 0.30$). Our results contrast to the results of a larger study on female polar bears from the Norwegian Arctic (Tartu et al., 2016). Tartu et al. (2016) conducted field work in both spring and autumn and measured $\delta^{15}\text{N}$ values in red blood cells (in which estimated half-life for $\delta^{15}\text{N}$ values is 3–4 months (Rode et al., 2016)) and the results suggested lower $\delta^{15}\text{N}$ values in northwestern Svalbard. These differences between our study and Tartu et al. (2016) may be due to the different seasons and matrixes covered in the two studies.

The capture position of the bears from the Russian Arctic did not explain the variation in THg levels based on GAM (*te*(Lat, Lon): $P = 0.48$, $r^2_{\text{adj}} = 0.05$). In addition, neither $\delta^{13}\text{C}$ nor $\delta^{15}\text{N}$ values were significant predictors for THg concentrations (Table 3B). However, values of $\delta^{13}\text{C}$ in the Russian subpopulations showed a decreasing trend towards the North (–0.34‰ per latitudinal step; $P < 0.001$), and a slightly increasing trend towards the East (0.027‰ per longitudinal step; $P < 0.001$; Figure 3). The fact that THg concentrations had no relation to either of the feeding habit proxies in the Russian bears (as opposed to e.g. the Norwegian bears from the present study and Lippold et al., 2020a (bears from the Barents Sea); McKinney et al., 2017 (bears from the Southern Beaufort Sea)) could potentially be related to the quality of the results, which was difficult to assure due to a limited number of samples used to determine analytical precision.

The observed $\delta^{13}\text{C}$ patterns in polar bears from the Russian Arctic, with values increasing towards the East and decreasing towards the North, may be related to the high influence of riverine input in that area, or to variation in $\delta^{13}\text{C}$ values in different sea water masses. Large rivers discharging into the western Russian Arctic contain high concentrations of dissolved

terrestrial organic carbon (Sonke et al., 2018), which have lower $\delta^{13}\text{C}$ values than carbon with marine origin (Fichot et al., 2013). In addition, coastal erosion from permafrost thawing might result in even higher terrestrial derived particulate organic carbon (POC) discharge than rivers, for instance along the East Siberian Arctic coast (Rachold et al., 2000; Vonk et al., 2012). Potentially, the slight increase of $\delta^{13}\text{C}$ values from west to east could be driven by the inflow of Atlantic water, in which $\delta^{13}\text{C}$ values are more depleted compared to the Arctic Basin (de la Vega et al., 2019). Values of $\delta^{13}\text{C}$ in CO_2 and POC in Arctic water bodies also decreased with increasing latitude, congruent with our observations in the Russian polar bear hair $\delta^{13}\text{C}$ (de la Vega et al., 2019). Latitudinal and longitudinal trends of $\delta^{15}\text{N}$ were not significant within the Russian polar bears (estimate for latitude: –0.07 per degree, $P = 0.13$; estimate for longitude: <0.003 per degree, $P = 0.36$).

Contrary to emission patterns, which are highest in East Asia (Zhang et al., 2016), THg concentrations were not higher in the Russian bears in closer geographical proximity than bears from the Barents Sea or more western Arctic. This is potentially because, according to modelling studies, Hg concentrations are relatively equally distributed in the atmosphere over the Russian Arctic, at levels comparable to the rest of the Arctic (Travnikov, 2005; Pacyna et al., 2016). Total Hg concentrations in polar bear hair from both the Norwegian and Russian Arctic were low compared to those reported in 2012–2016 for the Canadian Arctic (southern Beaufort Sea and Western Hudson Bay) or Greenland, which were up to 4-fold higher (Routti et al., 2019). An earlier study (2005–2008) reported very low THg concentrations in polar bear liver from the Chukchi/Bering Sea subpopulation, and exceptionally high concentrations (> 40 $\mu\text{g g}^{-1}$ wet weight) in bears from the southern and northern Beaufort Sea, which were attributed to a high Hg discharge from the Mackenzie River (Routti et al., 2011). Higher concentrations of THg in the southern Beaufort Sea subpopulation compared to the western Hudson Bay subpopulation have also been related to higher concentrations of pelagic MeHg and longer, more pelagic food web in the southern Beaufort Sea (St. Louis et al., 2011). Higher THg concentrations in polar bears from the Canadian Arctic and Greenland compared to those from the Norwegian and Russian Arctic do not seem to be related to the productivity of the shelf seas. Chukchi and Barents Seas are characterized as highly productive areas in contrast to interior shelf seas in the Russian and Canadian Arctic (Jin et al., 2012; Shen et al., 2018).

Data on Hg concentrations in any matrix from the Russian Arctic is not abundant but suggest that Hg concentrations in biota are generally lower in the Russian Arctic compared to the Canadian Arctic (e.g. Castello et al., 2014; Pomerleau et al., 2016; Pelletier et al., 2017). For example, THg

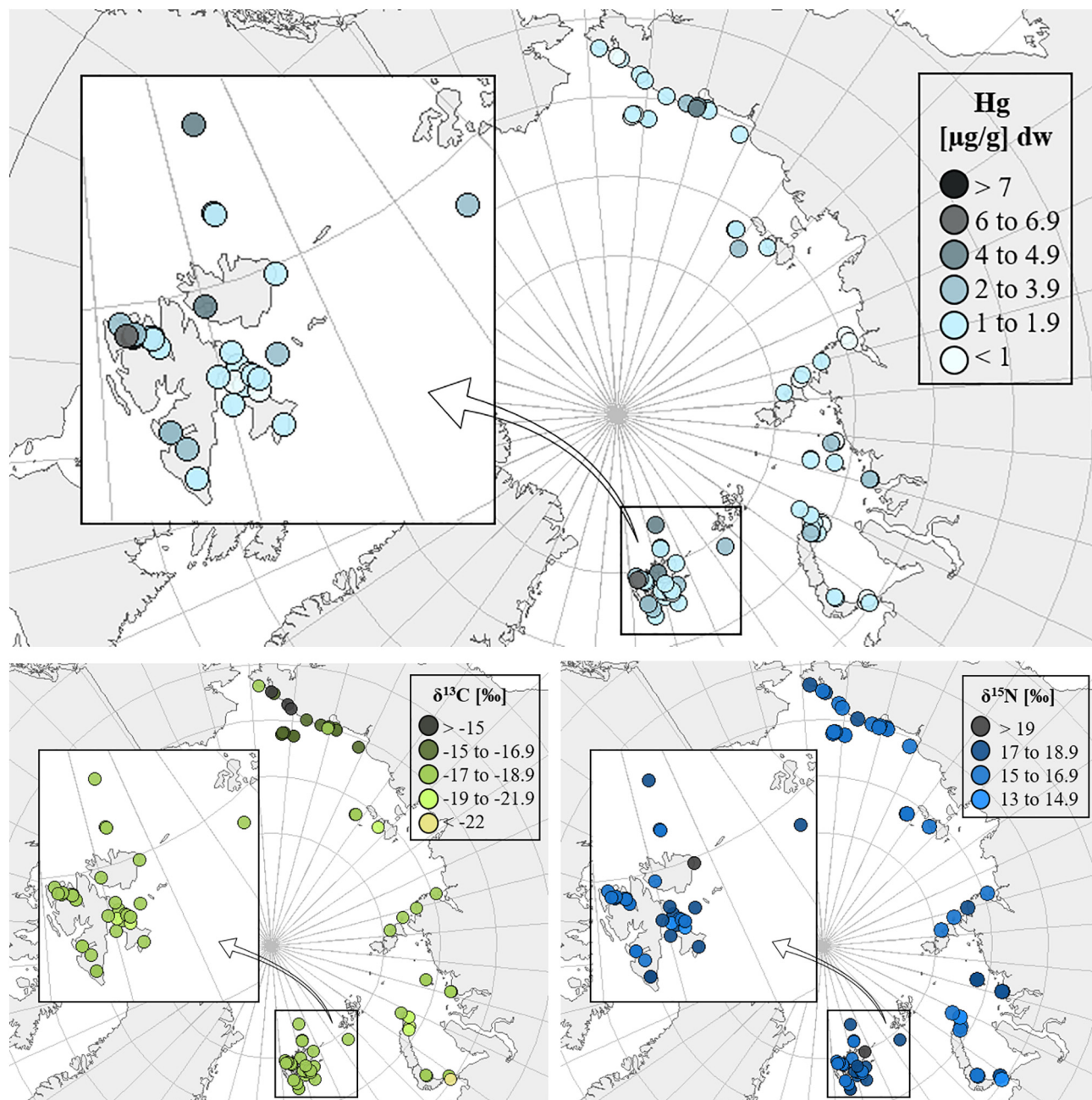


Fig. 2. Measured THg concentrations and stable isotope values ($\delta^{13}\text{C}$ and $\delta^{15}\text{N}$) in hair from individual bears captured on Svalbard, Norwegian Arctic, and in Russia. The median deviation in the results from the laboratories analyzing the Norwegian and Russian samples was $0.12 \mu\text{g g}^{-1} \text{ dw}$ for THg, 0.95‰ for $\delta^{13}\text{C}$, and 1.64‰ for $\delta^{15}\text{N}$; thus, the results should be compared with caution.

concentrations in fish from large rivers across the Russian Arctic were lower than in fish from the Canadian Mackenzie River, declined temporally (1980–2001) and spatially from west to east (Castello et al., 2014; Pelletier et al., 2017). Also, THg concentrations in livers of ringed seals (*Pusa hispida*) were highest in the western Canadian Arctic, and comparably low in ringed seals from Svalbard or the White Sea (Riget et al., 2005). In a circumpolar study on zooplankton, THg and MeHg concentrations were the highest in the southern Beaufort Sea, where biomagnification of MeHg from *Calanus* spp. to its predators was also greatest (Pomerleau et al., 2016). Circumpolar patterns of THg in polar bears did not reflect the circumpolar patterns of riverine THg fluxes, which were the highest in the river Lena that discharges in the Laptev Sea (Zolkos et al., 2020). This variation in riverine Hg discharge may reflect the magnitude of permafrost thaw presence and thaw in the divergent river basins (Schuster et al., 2018; Lim et al., 2019).

Atmospheric Hg concentrations from the western Russian Arctic were comparable with air concentrations from other Arctic locations (Golubeva et al., 2003); and similar to slightly lower than those measured in the Canadian Arctic (Steffen et al., 2005).

Global actions to reduce anthropogenic Hg release have been agreed upon at the “Minamata Convention on Mercury” in 2013 (<http://www.mercuryconvention.org>) to protect humans, biota, and the environment from the harmful effects of Hg. The Convention has been ratified by 123 parties, including Norway in 2017. Russia has signed, but not yet ratified, the Convention. Although Hg levels locally exceed maximum allowed limits close to hot spot emission points in Russia (Romanov et al., 2017; Pastukhov et al., 2019) that are mostly located below the Arctic circle (Kocman et al., 2013), it is seemingly not leading to high Hg exposure in polar bears from the Russian Arctic.

Mercury, Svalbard

Stable Isotopes, Svalbard

Stable Isotopes, Russia

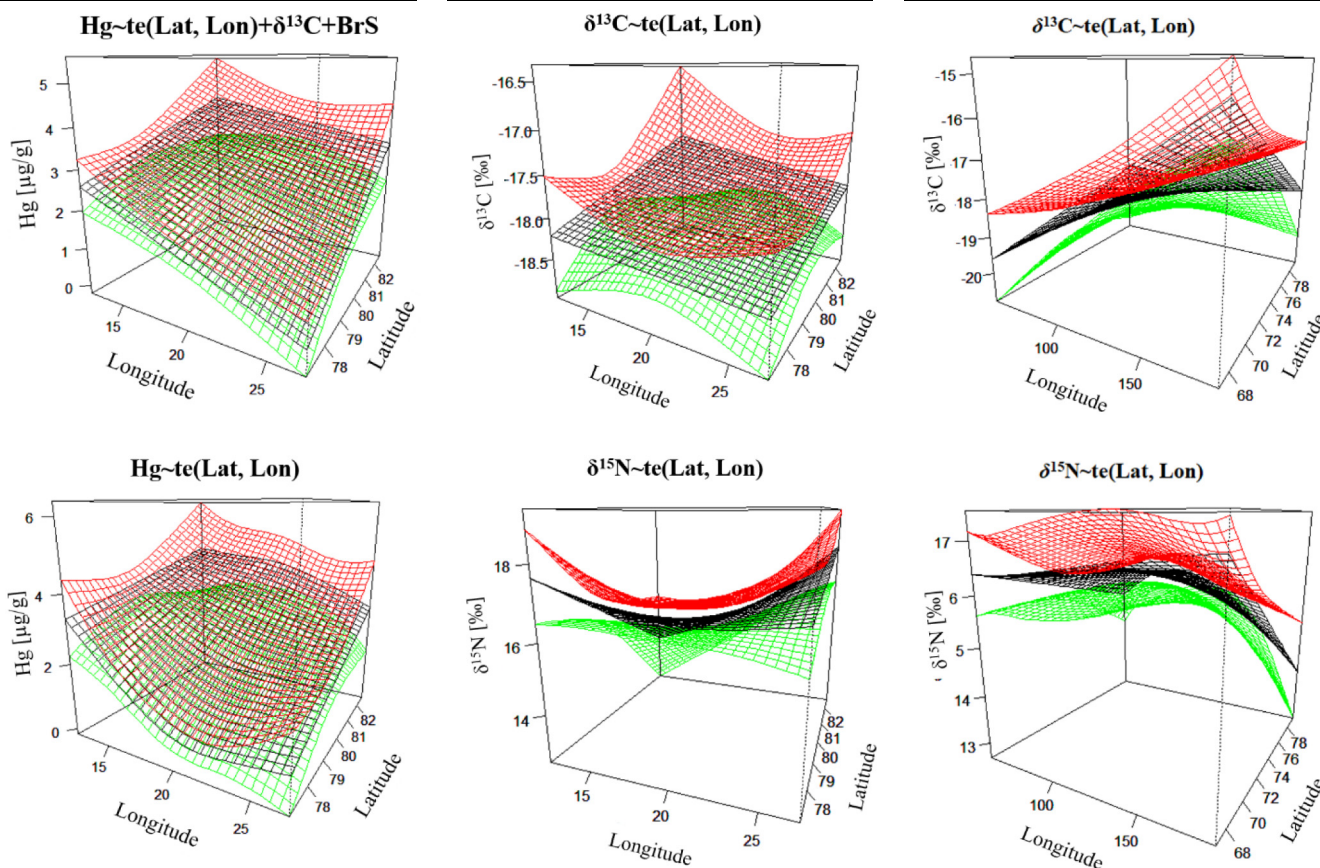


Fig. 3. Three-dimensional plots illustrating hair THg concentrations ($\mu\text{g g}^{-1}$ dw) as well as values of $\delta^{13}\text{C}$ and $\delta^{15}\text{N}$ (‰) in polar bears from the Svalbard Archipelago (left and middle), and Russia (right) estimated by generalized additive (mixed) models. The black grid lines show Hg concentrations or stable isotope values predicted by the model (see heading of each plot), while the red and green grid lines show the standard error. For Hg concentrations, the models with and without additional predictors ($\delta^{13}\text{C}$ and breeding status) are shown together for comparison. Model selection for the Russian data showed the null-model to be the best one, thus Hg concentrations predicted over the Russian Arctic are not shown.

Table 3

Model (GAMM) selection table (left) and averaged GAMM estimates (right; 95% CI in brackets) explaining the THg concentrations in Norwegian (A) and Russian polar bears (B) by centroid home range position, feeding ecology ($\delta^{13}\text{C}$, $\delta^{15}\text{N}$), breeding status (BrS; females with cubs of the year [COY] or yearling [Y] vs. solitary), body condition index (BCI), and age (Norwegian Arctic); or capture position and feeding ecology (Russian Arctic). The plus sign indicates that a smoothed or categorical variable was included in the model. Abbreviations: Int.: Intercept; te(Lat, Lon): smoothed latitude and longitude; df: degrees of freedom; AIC: Akaike Information Criterion; w: AIC weight. Estimates in bold are significant.

A) Norwegian Arctic: Model selection table										Model average	
Int.	te(Lat, Lon)	$\delta^{13}\text{C}$	$\delta^{15}\text{N}$	BrS	BCI	Age	df	ΔAIC	w	Int.	2.48 (1.91, 3.05)
2.51	+	0.36		+			11	0.00	0.760	$\delta^{13}\text{C}$	0.34 (0.16, 0.52)
2.11	+	0.31				0.05	10	4.41	0.084	$\delta^{15}\text{N}$	0.27 (0.06, 0.47)
2.58	+	0.31					9	4.53	0.079	Y	1.94 (-0.1, 3.98)
2.58	+	0.34			0.11		10	5.08	0.060	COY	-0.37(-1.01, 0.27)
2.40	+		0.28	+			11	10.1	0.005	BCI	0.1 (-0.19, 0.40)
2.57	+						8	10.2	0.005	Age	0.05 (-0.03, 0.12)
2.58	+		0.26				9	10.9	0.003		
2.15	+		0.29			0.04	10	11.5	0.002		
2.59	+		0.24		-0.07		10	12.2	0.002		
2.36							3	26.8	0.00		

B) Russian Arctic: Model Selection Table							Model Average	
Int.	te(Lat, Lon)	$\delta^{13}\text{C}$	$\delta^{15}\text{N}$	df	ΔAIC	w	Int.	1.72 (1.43, 2.01)
1.73				2	0.00	0.454	$\delta^{13}\text{C}$	-0.001 (-0.48, 0.36)
1.69	+		-1.19	8	1.05	0.269	$\delta^{15}\text{N}$	-0.19 (-0.48, 0.11)
1.69	+			7	1.63	0.201		
1.69	+	-0.001		8	3.56	0.077		

Table 4

Numbers of samples and summary statistics (GM: geometric mean; CI: confidence intervals) for THg concentrations ($\mu\text{g g}^{-1}$ dw) in hair from polar bears from different sub-populations.

	<i>n</i>		THg hair	Reference
Svalbard, Norway (2011–2016)	42	GM (95% CI)	2.20 (1.83–2.64)	This study
Kara Sea (2012–2016)	31	GM (95% CI)	1.09 (0.77–1.54)	This study
Laptev Sea (2014–2016)	7	GM (95% CI)	1.43 (0.88–2.32)	This study
Chukchi Sea (2008–2016)	20	GM (95% CI)	1.64 (1.30–2.06)	This study
Southern Beaufort Sea (2011)	15	GM (95% CI)	2.57 (1.93–3.42)	McKinney et al., 2017
Western Hudson Bay (2004–2016) ^a	590	~Mean	~4.7	Yurkowski et al., 2020
Baffin Bay (2009–2013)	124	Median (range)	6.0 (3.2–11.4)	Stern et al., 2021
East Greenland (2014–2017)	22	GM (95% CI)	7.22 (6.37–8.17)	Routti et al., 2019 (data from Rig�et et al., unpublished)

^a Mean of yearly averages; *n* varies among years (range 21–66).

4. Conclusions

We report concentrations of hair THg in polar bears throughout the Russian Arctic that are considerably lower compared to levels reported for North American and Greenlandic polar bear subpopulations. Within the Norwegian bears, levels tended to be higher in the Northwest compared to the Southeast, and higher THg levels with a higher proportion of marine prey and feeding at a higher trophic position. However, THg concentrations adjusted for feeding ecology and additionally breeding status showed similar spatial trends as the non-adjusted measured concentrations. In the Russian bears, THg concentrations varied little throughout the Russian Arctic, and were not significantly related to the bears' feeding ecology. Our study is one of few studies exploring Hg concentrations in the Russian Arctic. More studies on e.g. temporal trends of Hg in polar bears from the Russian Arctic are needed to monitor and understand the effectiveness of Hg emission regulations and the effect of climate change on Hg concentrations in the Arctic.

CRedit authorship contribution statement

Anna Lippold: Methodology, Formal analysis, Visualization, Writing - original draft, Writing - review & editing. **Andrei Boltunov:** Resources, Data curation, Writing - original draft, Funding acquisition. **Jon Aars:** Resources, Data curation, Writing - review & editing. **Magnus Andersen:** Resources, Data curation, Writing - review & editing. **Marie-Anne Blanchet:** Methodology, Writing - review & editing. **Rune Dietz:** Resources, Writing - review & editing. **Igor Eulaers:** Methodology, Writing - review & editing. **Tamara N. Morshina:** Resources, Methodology, Writing - original draft. **Vyacheslav S. Sevastyanov:** Resources, Methodology, Writing - original draft. **Jeffrey Welker:** Resources, Methodology, Writing - review & editing. **Heli Routti:** Conceptualization, Methodology, Writing - review & editing, Supervision, Project administration, Funding acquisition.

Declaration of competing interest

The authors declare that they have no known competing financial interests or personal relationships that could have appeared to influence the work reported in this paper.

Acknowledgements

We thank Anette Wold, Sophie Bourgeon, Annalis Brownlee, Matthew Rogers, Katelynn Johnson and Aaron Fisk for stable isotope analyses. The study was funded by the Ministry of Climate and Environment of Norway and the Norwegian Polar Institute. Additional funding for fieldwork was provided by the Centre for Ice, Climate and Environment (ICE) at the Norwegian Polar Institute and the World Wildlife Fund. The majority of samples from the Russian side were collected during contract work (Contractor – Arctic Research Centre LLC), whilst the remaining samples were obtained during other expeditions or as contributions from colleagues and partners. Funding for the Norwegian stable isotope analysis was

provided by a NSF Major Research Infrastructure award to JMW (0953271) that established the UAA Stable Isotope Facility and provided the mass spectrometer used to determine hair $\delta^{13}\text{C}$ and $\delta^{15}\text{N}$ values. JMW has also been supported during this research and publication construction phase by a Fulbright Distinguished Arctic Chairship-Norway and his UArctic Research Chairship. None of the funding sources had influence on any part of this research.

Appendix A. Supplementary data

Supplementary data to this article can be found online at <https://doi.org/10.1016/j.scitotenv.2022.153572>. The data show 1) correlation of latitude and longitude of capture positions with centroid home range positions of the Barents Sea polar bears and 2) list of candidate models and diagnostic and partial residual plots of GAM(M)s.

References

- AMAP, 2011. *AMAP Assessment 2011: Mercury in the Arctic*. Arctic Monitoring and Assessment Programme (AMAP), Oslo.
- Barton, K., 2019. *MuMIn: Multi-model Inference*. R Package Version 1.43.15.
- Bates, D., M achler, M., Bolker, B., Walker, S., 2015. Fitting linear mixed-effects models using lme4. *J. Stat. Softw.* 67, 1–51. <https://doi.org/10.18637/jss.v067.i01>.
- Bechshoft, T., Luo, Y., Bohart, A.M., Derocher, A.E., Richardson, E.S., Lunn, N.J., Pearson, D.G., 2020. Monitoring spatially resolved trace elements in polar bear hair using single spot laser ablation ICP-MS. *Ecol. Indic.* 119, 106822. <https://doi.org/10.1016/j.ecolind.2020.106822>.
- Becker, R.A., Wilks, A.R., Brownrigg, R., Minka, T.P., Deckmyn, A., 2018. *maps: Draw Geographical Maps*. R package version 3.3.0. <https://CRAN.R-project.org/package=maps>.
- Benoit, J.M., Gilmour, C.C., Heyes, A., Mason, R.P., Miller, C.L., 2002. Geochemical and biological controls over methylmercury production and degradation in aquatic ecosystems. *Biogeochemistry of Environmentally Important Trace Elements*. American Chemical Society, pp. 262–297. <https://doi.org/10.1021/bk-2003-0835.ch019>.
- Blanchet, M.A., Aars, J., Andersen, M., Routti, H., 2020. Space-use strategy affects energy requirements in Barents Sea polar bears. *Mar. Ecol. Prog. Ser.* 639, 1–19. <https://doi.org/10.3354/meps13290>.
- Born, E.W., Renzoni, A., Dietz, R., 1991. Total mercury in hair of polar bears (*Ursus maritimus*) from Greenland and Svalbard. *Polar Res.* 9, 113–120. <https://doi.org/10.3402/polar.v9i2.6784>.
- Braune, B., Norstrom, R.J., Wong, M.P., Collins, B.T., Lee, J., 1991. Geographical distribution of metals in livers of polar bears from the Northwest territories, Canada. *Sci. Total Environ.* 100, 283–299. [https://doi.org/10.1016/0048-9697\(91\)90381-N](https://doi.org/10.1016/0048-9697(91)90381-N).
- Braune, B.M., Outridge, P.M., Fisk, A.T., Muir, D.C., Helm, P.A., Hobbs, K., Hoekstra, P.F., Kuzyk, Z.A., Kwan, M., Letcher, R.J., Lockhart, W.L., Norstrom, R.J., Stern, G.A., Stirling, I., 2005. Persistent organic pollutants and mercury in marine biota of the Canadian Arctic: an overview of spatial and temporal trends. *Sci. Total Environ.* 351–352, 4–56. <https://doi.org/10.1016/j.scitotenv.2004.10.034>.
- Brun, C., Blanchet, M.-A., Ims, R., Aars, J., 2021. Stability of space use in Svalbard coastal female polar bears: intra-individual variability and influence of kinship. *Polar Res.* 40. <https://doi.org/10.33265/polar.v40.5355>.
- Castello, L., Zhulidov, A.V., Gurtovaya, T.Y., Robarts, R.D., Holmes, R.M., Zhulidov, D.A., Lysenko, V.S., Spencer, R.G., 2014. Low and declining mercury in arctic Russian rivers. *Environ. Sci. Technol.* 48, 747–752. <https://doi.org/10.1021/es403363v>.
- Cattet, M.R.L., Caulkett, N.A., Obbard, M.E., Stenhouse, G.B., 2002. A body-condition index for ursids. *Can. J. Zool.* 80, 1156–1161. <https://doi.org/10.1139/z02-103>.
- Christensen-Dalsgaard, S.N., Aars, J., Andersen, M., Lockyer, C., Yoccoz, N.G., 2009. Accuracy and precision in estimation of age of Norwegian Arctic polar bears (*Ursus maritimus*) using dental cementum layers from known-age individuals. *Polar Biol.* 33, 589–597. <https://doi.org/10.1007/s00300-009-0734-y>.
- Daase, M., Falk-Petersen, S., Varpe,  ., Darnis, G., S oreide, J.E., Wold, A., Leu, E., Berge, J., Philippe, B., Fortier, L., 2013. Timing of reproductive events in the marine copepod

- Calanus glacialis: a pan-Arctic perspective. *Can. J. Fish. Aquat. Sci.* 70, 871–884. <https://doi.org/10.1139/cjfas-2012-0401>.
- de la Vega, C., Jeffreys, R.M., Tuerena, R., Ganeshram, R., Mahaffey, C., 2019. Temporal and spatial trends in marine carbon isotopes in the Arctic Ocean and implications for food web studies. *Glob. Chang. Biol.* 25, 4116–4130. <https://doi.org/10.1111/gcb.14832>.
- Dietz, R., Letcher, R.J., Desforges, J.-P., Eulaers, I., Sonne, C., Wilson, S., Andersen-Ranberg, E., Basu, N., Barst, B.D., Bustnes, J.O., Bytingsvik, J., Ciesielski, T.M., Drevnick, P.E., Gabrielsen, G.W., Haarr, A., Hylland, K., Jessen, B.M., Levin, M., McKinney, M.A., Nørregaard, R.D., Pedersen, K.E., Provencher, J., Styrisshave, B., Tartu, S., Aars, J., Ackerman, J.T., Rosing-Asvid, A., Barrett, R., Bignert, A., Born, E.W., Branigan, M., Braune, B., Bryan, C.E., Dam, M., Eagles-Smith, C.A., Evans, M., Evans, T.J., Fisk, A.T., Gamber, M., Gustavson, K., Hartman, C.A., Helander, B., Herzog, M.P., Hoekstra, P.F., Houde, M., Hoydal, K., Jackson, A.K., Kucklick, J., Lie, E., Loseto, L., Mallory, M.L., Miljeteig, C., Mosbech, A., Muir, D.C.G., Nielsen, S.T., Peacock, E., Pedro, S., Peterson, S.H., Polder, A., Rigét, F.F., Roach, P., Saunes, H., Sinding, M.-H.S., Skaare, J.U., Søndergaard, J., Stenson, G., Stern, G., Treu, G., Schuur, S.S., Vikiingsson, G., 2019. Current state of knowledge on biological effects from contaminants on arctic wildlife and fish. *Sci. Total Environ.* 696, 133792. <https://doi.org/10.1016/j.scitotenv.2019.133792>.
- Dietz, R., Outridge, P.M., Hobson, K.A., 2009. Anthropogenic contributions to mercury levels in present-day Arctic animals—a review. *Sci. Total Environ.* 407, 6120–6131. <https://doi.org/10.1016/j.scitotenv.2009.08.036>.
- Dietz, R., Sonne, C., Basu, N., Braune, B., O'Hara, T., Letcher, R.J., Scheuhammer, T., Andersen, M., Andreasen, C., Andriashke, D., Asmund, G., Aubail, A., Baagoe, H., Born, E.W., Chan, H.M., Derocher, A.E., Grandjean, P., Knott, K., Kirkegaard, M., Krey, A., Lunn, N., Messier, F., Obbard, M., Olsen, M.T., Ostertag, S., Peacock, E., Renzoni, A., Rigét, F.F., Skaare, J.U., Stern, G., Stirling, I., Taylor, M., Wiig, O., Wilson, S., Aars, J., 2013. What are the toxicological effects of mercury in Arctic biota? *Sci. Total Environ.* 443, 775–790. <https://doi.org/10.1016/j.scitotenv.2012.11.046>.
- Elliott, K.H., Elliott, J.E., 2016. Origin of sulfur in diet drives spatial and temporal mercury trends in seabird eggs from Pacific Canada 1968–2015. *Environ. Sci. Technol.* 50, 13380–13386. <https://doi.org/10.1021/acs.est.6b05458>.
- Ficht, C.G., Kaiser, K., Hooker, S.B., Amon, R.M., Babin, M., Belanger, S., Walker, S.A., Benner, R., 2013. Pan-Arctic distributions of continental runoff in the Arctic Ocean. *Sci. Rep.* 3, 1053. <https://doi.org/10.1038/srep01053>.
- Fitzgerald, W.F., Lamborg, C.H., 2007. Geochemistry of mercury in the environment. In: Holland, H.D., Turekian, K.K. (Eds.), *Treatise on Geochemistry*, pp. 1–47.
- Golubeva, N., Burtseva, L., Matishov, G., 2003. Measurements of mercury in the near-surface layer of the atmosphere of the Russian Arctic. *Sci. Total Environ.* 306, 3–9. [https://doi.org/10.1016/S0048-9697\(02\)00480-1](https://doi.org/10.1016/S0048-9697(02)00480-1).
- Gongora, E., Braune, B.M., Elliott, K.H., 2018. Nitrogen and sulfur isotopes predict variation in mercury levels in Arctic seabird prey. *Mar. Pollut. Bull.* 135, 907–914. <https://doi.org/10.1016/j.marpolbul.2018.07.075>.
- Heimbürger, L.E., Sonke, J.E., Cossa, D., Point, D., Lagane, C., Laffont, L., Galfond, B.T., Nicolaus, M., Rabe, B., van der Loeff, M.R., 2015. Shallow methylmercury production in the marginal sea ice zone of the central Arctic Ocean. *Sci. Rep.* 5, 10318. <https://doi.org/10.1038/srep10318>.
- Jeremiason, J.D., Engstrom, D.R., Swain, E.B., Nater, E.A., Johnson, B.M., Almendinger, J.E., Monson, B.A., Kolk, R.K., 2006. Sulfate addition increases methylmercury production in an experimental wetland. *Environ. Sci. Technol.* 40, 380–3806. <https://doi.org/10.1021/es0524144>.
- Jin, M., Deal, C., Lee, S.H., Elliott, S., Hunke, E., Maltrud, M., Jeffery, N., 2012. Investigation of Arctic sea ice and ocean primary production for the period 1992–2007 using a 3-D global ice-ocean ecosystem model. *Deep Sea Res. II* 81–84, 28–35. <https://doi.org/10.1016/j.dsr.2.2011.06.003>.
- Kirk, J.L., Lehnher, I., Andersson, M., Braune, B.M., Chan, L., Dastoor, A.P., Dumford, D., Gleason, A.L., Loseto, L.L., Steffen, A., St Louis, V.L., 2012. Mercury in Arctic marine ecosystems: sources, pathways and exposure. *Environ. Res.* 119, 64–87. <https://doi.org/10.1016/j.envres.2012.08.012>.
- Lehnher, I., 2014. Methylmercury biogeochemistry: a review with special reference to Arctic aquatic ecosystems. *Environ. Rev.* 22, 229–243. <https://doi.org/10.1139/er-2013-0059>.
- Lim, A.G., Sonke, J.E., Krickov, I.V., Manasyrov, R.M., Loiko, S.V., Pokrovsky, O.S., 2019. Enhanced particulate Hg export at the permafrost boundary, western Siberia. *Environ. Pollut.* 254, 113083. <https://doi.org/10.1016/j.envpol.2019.113083>.
- Lippold, A., Aars, J., Andersen, M., Aubail, A., Derocher, A., Dietz, R., Eulaers, I., Sonne, C., Welker, J.M., Wiig, O., Routti, H., 2020a. Two decades of mercury concentrations in Barents Sea polar bears (*Ursus maritimus*) in relation to dietary carbon, sulfur, and nitrogen. *Environ. Sci. Technol.* 54, 7388–7397. <https://doi.org/10.1021/acs.est.0c01848>.
- Lippold, A., Aars, J., Andersen, M., Aubail, A., Derocher, A., Dietz, R., Eulaers, I., Sonne, C., Welker, J.M., Wiig, Ø., Routti, H., 2020b. Concentrations of Mercury And Stable Isotope Values of Carbon, Sulfur And Nitrogen in Polar Bear Hair From the Barents Sea in 1995–2016 [Data set]. Norwegian Polar Institute <https://doi.org/10.21334/npolar.2020.9ae3d26e>.
- Mauritzen, M., Derocher, A.E., Wiig, Ø., 2001. Space-use strategies of female polar bears in a dynamic sea ice habitat. *Can. J. Zool.* 79, 1704–1713. <https://doi.org/10.1139/z01-126>.
- McIlroy, D., 2018. Packaged for R by Ray Brownrigg. Thomas P Minka and transition to Plan 9 codebase by Roger Bivand. 2018. mapproj: Map Projections. R package version 1.2.6. <https://CRAN.R-project.org/package=mapproj>.
- McKinney, M.A., Atwood, T.C., Pedro, S., Peacock, E., 2017. Ecological change drives a decline in mercury concentrations in southern Beaufort Sea polar bears. *Environ. Sci. Technol.* 51, 7814–7822. <https://doi.org/10.1021/acs.est.7b00812>.
- Mohr, C.O., 1947. Table of equivalent populations of north American small mammals. *Am. Midl. Nat.* 37, 223–249. <https://doi.org/10.2307/2421652>.
- Muir, D., Braune, B., DeMarch, B., Norstrom, R.J., Wagemann, R., Lockhart, W.L., Hargrave, B.T., Bright, D., Addison, R., Payne, J., Reimer, K., 1999. Spatial and temporal trends and effects of contaminants in the Canadian Arctic marine ecosystem: a review. *Sci. Total Environ.* 230, 83–144. [https://doi.org/10.1016/S0048-9697\(99\)00037-6](https://doi.org/10.1016/S0048-9697(99)00037-6).
- Norstrom, R.J., Schweinsberg, R.E., Collins, B.T., 1986. Heavy metals and essential elements in livers of the polar bear (*Ursus maritimus*) in the Canadian Arctic. *Sci. Total Environ.* 48, 195–212. [https://doi.org/10.1016/S0048-9697\(86\)80005-5](https://doi.org/10.1016/S0048-9697(86)80005-5).
- Outridge, P.M., Mason, R.P., Wang, F., Guerrero, S., Heimbürger-Boavida, L.E., 2018. Updated global and oceanic mercury budgets for the united nations global mercury assessment 2018. *Environ. Sci. Technol.* 52, 11466–11477. <https://doi.org/10.1021/acs.est.8b01246>.
- Pacyna, J.M., Travnikov, O., De Simone, F., Hedgecock, I.M., Sundseth, K., Pacyna, E.G., Steenhuisen, F., Pirrone, N., Munthe, J., Kindbom, K., 2016. Current and future levels of mercury atmospheric pollution on a global scale. *Atmos. Chem. Phys.* 16, 12495–12511. <https://doi.org/10.5194/acp-16-12495-2016>.
- Pastukhov, M.V., Poletaeva, V.I., Tirkikh, E.N., 2019. Long-term dynamics of mercury pollution of the Bratsk reservoir bottom sediments, Baikal region, Russia. *IOP Conf. Ser.: Earth Environ. Sci.* 321. <https://doi.org/10.1088/1755-1315/321/1/012041>.
- Pelletier, A.R., Castello, L., Zhulidov, A.V., Gurtovaya, T.Y., Roberts, R.D., Holmes, R.M., Zhulidov, D.A., Spencer, R.G.M., 2017. Temporal and longitudinal mercury trends in burbot (*Lota lota*) in the Russian Arctic. *Environ. Sci. Technol.* 51, 13436–13442. <https://doi.org/10.1021/acs.est.7b03929>.
- Pinheiro, J., Bates, D., DebRoy, S., Sarkar, D., Team, R.C., 2019. nlme: Linear and Nonlinear Mixed Effects Models. R package version 3.1-131. <https://CRAN.R-project.org/package=nlme>.
- Polar Bear Range States, 2015. Circumpolar Action Plan: Conservation Strategy for Polar Bears. A product of the representatives of the parties to the 1973 Agreement on the Conservation of Polar Bears. <https://polarbearagreement.org/resources/agreement/circumpolar-action-plan/circumpolar-action-plan>.
- Pomerleau, C., Stern, G.A., Pučko, M., Foster, K.L., Macdonald, R.W., Fortier, L., 2016. Pan-Arctic concentrations of mercury and stable isotope ratios of carbon ($\delta^{13}C$) and nitrogen ($\delta^{15}N$) in marine zooplankton. *Sci. Total Environ.* 551–552, 92–100. <https://doi.org/10.1016/j.scitotenv.2016.01.172>.
- R Core Team, 2019. R: A Language And Environment for Statistical Computing. R Foundation for Statistical Computing, Vienna, Austria <https://www.R-project.org/>.
- Rachold, V., Grigoriev, M.N., Are, F.E., Solomon, S., Reimnitz, E., Kassens, H., Antonow, M., 2000. Coastal erosion vs riverine sediment discharge in the Arctic Shelf seas. *Int. J. Earth Sci.* 89, 450–460. <https://doi.org/10.1007/s005310000113>.
- Renzoni, A., Norstrom, R.J., 1990. Mercury in the hairs of polar bears *Ursus maritimus*. *Polar Rec.* 26. <https://doi.org/10.1017/S003224740001192X>.
- Riget, F., Muir, D., Kwan, M., Savinova, T., Nyman, M., Woshner, V., O'Hara, T., 2005. Circumpolar pattern of mercury and cadmium in ringed seals. *Sci. Total Environ.* 351–352, 312–322. <https://doi.org/10.1016/j.scitotenv.2004.05.032>.
- Rode, K.D., Stricker, C.A., Erlenbach, J., Robbins, C.T., Cherry, S.G., Newsome, S.D., Cutting, A., Jensen, S., Stenhouse, G., Brooks, M., Hash, A., Nicassio, N., 2016. Isotopic incorporation and the effects of fasting and dietary lipid content on isotopic discrimination in large carnivorous mammals. *Physiol. Biochem. Zool.* 89, 182–197. <https://doi.org/10.1086/686490>.
- Rogers, M.C., Peacock, E., Simac, K., O'Dell, M.B., Welker, J.M., 2015. Diet of female polar bears in the southern Beaufort Sea of Alaska: evidence for an emerging alternative foraging strategy in response to environmental change. *Polar Biol.* 38, 1035–1047. <https://doi.org/10.1007/s00300-015-1665-4>.
- Romanov, A.V., Ignatieva, Y.S., Morozova, I.A., Speranskaya, O.A., Tsitser, O.Y., 2017. Mercury pollution in Russia: problems and recommendations. *Univ. environment*. http://www.ecoaccord.org/pop/Rtutnoe_zagryaznenie_English_25-08.pdf.
- Routti, H., Atwood, T.C., Bechshoft, T., Boltunov, A., Ciesielski, T.M., Desforges, J.P., Dietz, R., Gabrielsen, G.W., Jessen, B.M., Letcher, R.J., McKinney, M.A., Morris, A.D., Rigét, F.F., Sonne, C., Styrisshave, B., Tartu, S., 2019. State of knowledge on current exposure, fate and potential health effects of contaminants in polar bears from the circumpolar Arctic. *Sci. Total Environ.* 664, 1063–1083. <https://doi.org/10.1016/j.scitotenv.2019.02.030>.
- Routti, H., Letcher, R., Born, E., Branigan, M., Dietz, R., Evans, T.J., McKinney, M.A., Peacock, E., Sonne, C., 2012. Influence of carbon and lipid sources on variation of mercury and other trace elements in polar bears (*Ursus maritimus*). *Environ. Toxicol. Chem.* 31, 2739–2747. <https://doi.org/10.1002/etc.2005>.
- Routti, H., Letcher, R.J., Born, E.W., Branigan, M., Dietz, R., Evans, T.J., Fisk, A.T., Peacock, E., Sonne, C., 2011. Spatial and temporal trends of selected trace elements in liver tissue from polar bears (*Ursus maritimus*) from Alaska, Canada and Greenland. *J. Environ. Monit.* 13, 2260–2267. <https://doi.org/10.1039/c1em10088b>.
- Routti, H., Lippold, A., Boltunov, A., Aars, J., Andersen, M., Blanchet, M., Dietz, R., Eulaers, I., Morshina, T., Sevastyanov, V., Welker, J., 2021. Concentrations of Mercury And Stable Isotope Values of Carbon And Nitrogen in Polar Bear Hair From the Norwegian And Russian Arctic [Data set]. Norwegian Polar Institute <https://doi.org/10.21334/npolar.2021.296a5c63>.
- Rush, S.A., Borga, K., Dietz, R., Born, E.W., Sonne, C., Evans, T., Muir, D.C., Letcher, R.J., Norstrom, R.J., Fisk, A.T., 2008. Geographic distribution of selected elements in the livers of polar bears from Greenland, Canada and the United States. *Environ. Pollut.* 153, 618–626. <https://doi.org/10.1016/j.envpol.2007.09.006>.
- Schartup, A.T., Soerensen, A.L., Heimbürger-Boavida, L.E., 2020. Influence of the Arctic sea-ice regime shift on sea-ice methylated mercury trends. *Environ. Sci. Technol. Lett.* 7, 708–713. <https://doi.org/10.1021/acs.estlett.0c00465>.
- Schloerke, B., Crowley, J., Cook, D., Briatte, F., Marbach, M., Thoen, E., Elberg, A., Larmarange, J., 2018. GGally: Extension to 'ggplot2'. R package version 1. <https://CRAN.R-project.org/package=nlme> <https://cran.r-project.org/web/packages/GGally/>.
- Schuster, P.F., Schaefer, K.M., Aiken, G.R., Antweiler, R.C., Dewild, J.F., Gryziec, J.D., Gusmeroli, A., Hugelius, G., Jafarov, E., Krabbenhoft, D.P., Liu, L., Herman-Mercer, N., Mu, C., Roth, D.A., Schaefer, T., Striegl, R.G., Wickland, K.P., Zhang, T., 2018. Permafrost stores a globally significant amount of mercury. *Geophys. Res. Lett.* 45, 1463–1471. <https://doi.org/10.1002/2017gl075571>.

- Shen, Y., Benner, R., Kaiser, K., Fichot, C.G., Whitedge, T.E., 2018. Pan-Arctic distribution of bioavailable dissolved organic matter and linkages with productivity in ocean margins. *Geophys. Res. Lett.* 45, 1490–1498. <https://doi.org/10.1002/2017GL076647>.
- Soerensen, A.L., Jacob, D.J., Schartup, A.T., Fisher, J.A., Lehnerr, I., St. Louis, V.L., Heimbürger, L.-E., Sonke, J.E., Krabbenhoft, D.P., Sunderland, E.M., 2016. A mass budget for mercury and methylmercury in the Arctic Ocean. *Glob. Biogeochem. Cycles* 30, 560–575. <https://doi.org/10.1002/2015gb005280>.
- Sonke, J.E., Teisserenc, R., Heimbürger-Boavida, L.-E., Petrova, M.V., Maruszczak, N., Le Dantec, T., Chupakov, A.V., Li, C., Thackray, C.P., Sunderland, E.M., Tananaev, N., Pokrovsky, O.S., 2018. Eurasian river spring flood observations support net Arctic Ocean mercury export to the atmosphere and Atlantic Ocean. *Proc. Natl. Acad. Sci. U. S. A.* 115, E11586–E11594. <https://doi.org/10.1073/pnas.1811957115>.
- Steffen, A., Schroeder, W., Macdonald, R., Poissant, L., Konoplev, A., 2005. Mercury in the Arctic atmosphere: an analysis of eight years of measurements of GEM at Alert (Canada) and a comparison with observations at Amderma (Russia) and Kuujuaarapik (Canada). *Sci. Total Environ.* 342, 185–198. <https://doi.org/10.1016/j.scitotenv.2004.12.048>.
- St. Louis, V.L., Derocher, A.E., Stirling, I., Graydon, J.A., Lee, C., Jocksch, E., Richardson, E., Ghorpade, S., Kwan, A.K., Kirk, J.L., Lehnerr, I., Swanson, H.K., 2011. Differences in mercury bioaccumulation between polar bears (*Ursus maritimus*) from the Canadian high- and sub-Arctic. *Environ. Sci. Technol.* 45, 5922–5928. <https://doi.org/10.1021/es2000672>.
- Stern, G.A., Macdonald, R.W., Outridge, P.M., Wilson, S., Chetelat, J., Cole, A., Hintelmann, H., Loseto, L.L., Steffen, A., Wang, F., Zdanowicz, C., 2012. How does climate change influence Arctic mercury? *Sci. Total Environ.* 414, 22–42. <https://doi.org/10.1016/j.scitotenv.2011.10.039>.
- Stern, J.H., Laidre, K.L., Born, E., Wiig, Ø., Sonne, C., Dietz, R., Fisk, A., McKinney, M.A., 2021. Feeding habits of Baffin Bay polar bears (*Ursus maritimus*): insight from stable isotopes and total mercury in hair. *Mar. Ecol. Prog. Ser.* 677. <https://doi.org/10.3354/meps13864>.
- Stirling, I., Spencer, C., Andriashek, D., 1989. Immobilization of polar bears (*Ursus maritimus*) with Telazol® in the Canadian Arctic. *J. Wildl. Dis.* 25, 159–168. <https://doi.org/10.7589/0090-3558-25.2.159>.
- Tartu, S., Aars, J., Andersen, M., Polder, A., Bourgeon, S., Merkel, B., Lowther, A.D., Bytingsvik, J., Welker, J.M., Derocher, A., Jenssen, B.M., Routti, H., 2018. Choose your poison - space-use strategy influences pollutant exposure in Barents Sea polar bears. *Environ. Sci. Technol.* 52, 3211–3221. <https://doi.org/10.1021/acs.est.7b06137>.
- Tartu, S., Bourgeon, S., Aars, J., Andersen, M., Ehrlich, D., Thiemann, G.W., Welker, J.M., Routti, H., 2016. Geographical area and life history traits influence diet in an arctic marine predator. *PLoS One* 11, e0155980. <https://doi.org/10.1371/journal.pone.0155980>.
- Travnikov, O., 2005. Contribution of the intercontinental atmospheric transport to mercury pollution in the Northern Hemisphere. *Atmos. Environ.* 39, 7541–7548. <https://doi.org/10.1016/j.atmosenv.2005.07.066>.
- UN Environment, 2019. *Global Mercury Assessment 2018*. UN Environment Programme, Chemicals and Health Branch, Geneva, Switzerland <https://www.unep.org/resources/publication/global-mercury-assessment-2018>.
- Vonk, J.E., Sanchez-Garcia, L., van Dongen, B.E., Alling, V., Kosmach, D., Charkin, A., Semiletov, I.P., Dudarev, O.V., Shakhova, N., Roos, P., Eglinton, T.I., Andersson, A., Gustafsson, O., 2012. Activation of old carbon by erosion of coastal and subsea permafrost in Arctic Siberia. *Nature* 489, 137–140. <https://doi.org/10.1038/nature11392>.
- Wang, K., Munson, K.M., Beaupre-Laperriere, A., Mucci, A., Macdonald, R.W., Wang, F., 2018. Subsurface seawater methylmercury maximum explains biotic mercury concentrations in the Canadian Arctic. *Sci. Rep.* 8, 14465. <https://doi.org/10.1038/s41598-018-32760-0>.
- Wickham, H., 2016. *ggplot2: Elegant Graphics for Data Analysis*. Springer-Verlag, New York.
- Wood, S., 2018. mgcv: Mixed GAM Computation Vehicle with Automatic Smoothness Estimation R package version 1.8-23. <https://CRAN.R-project.org/package=mgcv>.
- Yurkowski, D.J., Richardson, E.S., Lunn, N.J., Muir, D.C.G., Johnson, A.C., Derocher, A.E., Ehrman, A.D., Houde, M., Young, B.G., Debets, C.D., Sciuillo, L., Thiemann, G.W., Ferguson, S.H., 2020. Contrasting temporal patterns of mercury, niche dynamics, and body fat indices of polar bears and ringed seals in a melting icescape. *Environ. Sci. Technol.* 54, 2780–2789. <https://doi.org/10.1021/acs.est.9b06656>.
- Zhang, Y., Jacob, D.J., Horowitz, H.M., Chen, L., Amos, H.M., Krabbenhoft, D.P., Slemr, F., St. Louis, V.L., Sunderland, E.M., 2016. Observed decrease in atmospheric mercury explained by global decline in anthropogenic emissions. *PNAS* 113, 526–531. <https://doi.org/10.1073/pnas.1516312113>.
- Zhang, Y., Soerensen, A.L., Schartup, A.T., Sunderland, E.M., 2020. A global model for methylmercury formation and uptake at the base of marine food webs. *Glob. Biogeochem. Cycles* 34. <https://doi.org/10.1029/2019gb006348>.
- Zolkos, S., Krabbenhoft, D.P., Suslova, A., Tank, S.E., McClelland, J.W., Spencer, R.G.M., Shiklomanov, A., Zhulidov, A.V., Gurtovaya, T., Zimov, N., Zimov, S., Mutter, E.A., Kutny, L., Amos, E., Holmes, R.M., 2020. Mercury export from Arctic great rivers. *Environ. Sci. Technol.* 54, 4140–4148. <https://doi.org/10.1021/acs.est.9b07145>.